

A Method for the Analysis of Respiratory Sinus Arrhythmia Using Continuous Wavelet Transforms

Laurence Cnockaert, *Student Member, IEEE*,

Pierre-François Migeotte, Lise Daubigny,

G. Kim Prisk, *Senior Member, IEEE*,

Francis Grenez, *Member, IEEE*, and Rui Carlos Sá*, *Member, IEEE*

Abstract—A continuous wavelet transform-based method is presented to study the nonstationary strength and phase delay of the respiratory sinus arrhythmia (RSA). The RSA is the cyclic variation of instantaneous heart rate at the breathing frequency. In studies of cardio-respiratory interaction during sleep, paced breathing or postural changes, low respiratory frequencies, and fast changes can occur. Comparison on synthetic data presented here shows that the proposed method outperforms traditional short-time Fourier-transform analysis in these conditions. On the one hand, wavelet analysis presents a sufficient frequency-resolution to handle low respiratory frequencies, for which time frames should be long in Fourier-based analysis. On the other hand, it is able to track fast variations of the signals in both amplitude and phase for which time frames should be short in Fourier-based analysis.

Index Terms—Cardio-respiratory interaction, continuous wavelet transform (CWT), heart rate variability (HRV), respiratory sinus arrhythmia (RSA).

I. INTRODUCTION

The heart rate variability (HRV) is traditionally divided in very low frequency (VLF), low frequency (LF), and high frequency (HF) components, the frequency bands of which are, respectively, [0.003 Hz, 0.04 Hz], [0.04 Hz, 0.15 Hz] and [0.15 Hz, 0.5 Hz] [1]. In the HF band, an oscillation can usually be observed at the breathing frequency. It is called the respiratory sinus arrhythmia (RSA). The study of the RSA has produced extensive literature both concerning its causes [2], [3], and the methodology to determine it [1]. It is generally accepted that RSA amplitude is a noninvasive marker of the activity of the parasympathetic nervous system [3], [4], and can therefore be used to infer relative changes in parasympathetic cardiac tone. The RSA phase delay is a measure of the time delay between respiratory cycles and RSA. It is an indirect, noninvasive measure of the integration time of the cardio-respiratory interaction, and can be estimated by frequency [5], [6] as well as time-domain methods [7].

Dynamic analysis of HRV is traditionally performed by means of short-time Fourier transform (STFT), following established guide-

lines [1]. However, STFT analysis is limited by its time–frequency resolution tradeoff: a long window gives a better frequency resolution, and a short window a better time resolution. The window-length optimization is difficult for short or nonstationary time series. In these cases, outputs are averaged over different states or conditions, and transients blurred. Therefore, nonstationary spectral methods have been implemented, based on time-variant autoregressive models [8], Wigner–Ville distribution [8], [9], selective discrete Fourier transform [10], or discrete or continuous wavelet transform, using various mother wavelets (e.g., Daubechies 4 [11], harmonic wavelet [12]).

The aim of this brief is to present an analysis method of the cardio-respiratory interaction based on continuous wavelet transforms (CWTs). It is compared to STFT analysis on synthetic data, with a view to handle low breathing frequencies and fast variations. This is of particular relevance in the study of RSA dynamics during sleep, where respiratory frequencies below 0.2 Hz (e.g., [13]) occur simultaneously to fast variations in RSA, due to changes in sleep stage and corresponding sympatho-vagal balance [14]. Sudden RSA changes, accompanied by low breathing frequencies, are also present in paced breathing protocols [7] and postural changes (tilt) experiments [8], [10].

II. METHODS

A. Algorithm

The algorithm calculates the gain and phase delay of the RSA based on CWTs. The analysis is limited to time intervals where the estimated respiratory frequency and the estimated frequency of the main peak in the HF band of HRV are equal within ± 0.02 Hz.

Continuous wavelet transform analysis: The time-dependent power spectra of the respiratory and HRV signal are calculated by means of CWTs.

The CWT of a signal $x(t)$ is defined as

$$\text{CWT}(t, \lambda) = \int_{-\infty}^{+\infty} x(u) \frac{1}{\sqrt{\lambda}} \psi^* \left(\frac{u-t}{\lambda} \right) du \quad (1)$$

where $\psi(t)$ is the mother wavelet and $\text{CWT}(\lambda, t)$ the wavelet transform coefficient for scale λ at time t . The time- and frequency resolution of the wavelet $\psi_\lambda(t)$ are defined as $4\sigma_t$ and $4\sigma_f$, respectively. σ_t and σ_f are the standard deviation of $|\psi_\lambda(t)|^2$ and $|\hat{\psi}_\lambda(f)|^2$, where $\psi_\lambda(t) = (1/\sqrt{\lambda})\psi(u-t)/\lambda$ and $\hat{\cdot}$ symbolizes the Fourier transform.

The amplitude and phase of the complex CWT coefficients obtained using an analytical mother wavelet are estimates of the envelope and instantaneous phase of the spectral components of the signal in the frequency-band centered on the central frequency of the wavelet [15]. Here, the complex Morlet wavelet [15] is used because it is a Gaussian-shaped analytical wavelet. This shape optimizes the product of the time- and frequency resolutions of the wavelet.

The time resolution in the HF band should be close to 30 sec, the duration of standard sleep stage scoring windows. On the other hand, the frequency resolution in the VLF and LF bands should be optimized. To satisfy both criteria, parameter f_0 , the central frequency of the Morlet mother wavelet, is set to $15/2\pi$ Hz in this study. The time resolution then varies from 45 to 14 sec in the HF band, and the frequency resolution varies from 7 to 28 mHz in the LF band.

From the CWT of the respiratory volume signal, the respiratory frequency $f_{\text{resp}}(t)$ is estimated by the frequency corresponding to the maximal CWT amplitude for each time step. The corresponding phase $\Phi_{\text{resp}}(t)$ is given by the CWT phase at frequency $f_{\text{resp}}(t)$. The energy $E_{\text{resp}}(t)$ is estimated by the surface of the peak, using a Gaussian approximation of the peak's shape. The frequency $f_{\text{HF}}(t)$,

Manuscript received October 31, 2007; revised January 2008. This work was supported by the Program of Development of Experiments (PRODEX), managed by the European Space Agency in collaboration with the Belgian Federal Science Policy Office. Asterisk indicates the corresponding author.

L. Cnockaert is with the “Laboratoires d’Images, Signaux et Dispositifs de Télécommunications,” Faculté des Sciences Appliquées, Université Libre de Bruxelles (U.L.B.), 1050 Brussels, Belgium, and also with the *Fonds pour la Formation a la Recherche dans l’Industrie et dans l’Agriculture*, B-1000, Bruxelles, Belgium.

P.-F. Migeotte is with the Signal and Image Center, Royal Military Academy, B-1000 Brussels, Belgium.

L. Daubigny is with the NXP Semiconductors, B-3001 Leuven, Belgium.

G. K. Prisk is with the Physiology National Aeronautics and Space Administration (NASA) Laboratory, Department of Medicine, University of California, San Diego, CA 92093-0931 USA.

F. Grenez is with the “Laboratoires d’Images, Signaux et Dispositifs de Télécommunications,” Faculté des Sciences Appliquées, Université Libre de Bruxelles (U.L.B.), 1050 Brussels, Belgium.

*R. C. Sá is with the “Laboratoire de Physique Biomédicale,” Université Libre de Bruxelles (U.L.B.), B-1070 Brussels, Belgium (e-mail: rui.carlos.sa@ulb.ac.be).

Digital Object Identifier 10.1109/TBME.2008.918576

corresponding phase $\Phi_{\text{HF}}(t)$ and energy $E_{\text{HF}}(t)$ of the HF peak of the HRV signal is estimated in a similar way from the CWT of the HRV signal in the HF band.

The amplitude ratio (AR) and phase delay (in seconds) between the respiratory signal and RSA component of the HRV signal are given by $\text{AR}(t) = E_{\text{HF}}(t)/E_{\text{resp}}(t)$ and $\Delta\Phi_t(t) = (\Phi_{\text{resp}}(t) - \Phi_{\text{HF}}(t))/2\pi f_{\text{resp}}$.

B. Synthetic Data

Synthetic cardiac and respiratory data with varying phase, amplitude, and frequency are created to test the algorithm, and to compare it to STFT-based algorithms.

The respiratory volume signal $S_{\text{resp}}(t)$ is synthesized by means of a sinusoid of frequency f_{resp} , amplitude a_1 , and phase Φ_{t0} , to which white noise was added (2). All parameters can vary in time, corresponding to changes in breathing frequencies, tidal volume, and phase drifts or “resets” of the respiratory cycle.

Instantaneous heart period variability, represented by the uniformly resampled RR-interval time series $S_{\text{URRI}}(t)$, is synthesized by summing a constant b_0 (representing the average heart beat interval) with three sinusoids of amplitudes b_{VLF} , b_{LF} , b_{HF} , and of frequencies f_{VLF} , f_{LF} , f_{HF} (3). Because the HF component represents the RSA, f_{HF} is set equal to f_{resp} . A phase parameter $\Phi_{t0} + \Delta\Phi_t$ is added in the HF component to model the phase difference between heart rate and respiratory signals. White noise is added to the phase and to the signal.

The synthetic respiratory and heart-rate interval signals are thus given by

$$S_{\text{resp}}(t) = a_1 \cos(2\pi f_{\text{resp}}(t + \Phi_{t0})) + \text{noise}(t) \quad (2)$$

$$\begin{aligned} S_{\text{URRI}}(t) = & b_0 + b_{\text{VLF}} \cos(2\pi f_{\text{VLF}} t) + b_{\text{LF}} \cos(2\pi f_{\text{LF}} t) \\ & + b_{\text{HF}} \cos(2\pi f_{\text{resp}}(t + \Phi_{t0} + \Delta\Phi_t + \text{noise}_{\Phi}(t))) \\ & + \text{noise}(t). \end{aligned} \quad (3)$$

III. RESULTS

The performance of the CWT-based algorithm is compared to the results obtained via short-time Fourier transform-based methods, using 30 and 120 sec long Hamming windows, *STFT30* and *STFT120*. To study the dynamics of the cardio-respiratory interaction, the major limitations arise from the ability of the method to detect the RSA peak, and to track fast changes. Noise is not a major issue, because the interpolated instantaneous heart period (*RR*-interval) time series used in HRV analysis usually presents low noise levels [1]. Therefore, the algorithms are compared with regard to the value of the respiratory frequency and to time-varying phase delays.

1) *Time-varying respiratory frequency*: The sensitivity of the methods to respiratory frequency changes is evaluated on synthetic data with a sinusoidally modulated respiratory frequency. The variation range covers the frequency interval of normal breathing [0.15 Hz, 0.35 Hz]. $f_{\text{resp}}(t) = \overline{f_{\text{resp}}}(1 + A_{\text{mod}} \cos(2\pi f_{\text{mod}} t))$, where $\overline{f_{\text{resp}}} = 0.25$ Hz, $A_{\text{mod}} = 0.4$, and $f_{\text{mod}} = 0.0025$ Hz. The two LF components of the URRI signal are modeled by a unique peak at 0.1 Hz. The other parameters of (2) and (3) are $a_1 = 0.2$, $b_0 = 1$ sec, $b_{\text{VLF}} = 0$, $b_{\text{LF}} = 0.06$ sec, $f_{\text{LF}} = 0.1$ Hz, $b_{\text{HF}} = 0.03$ sec, $\Phi_{t0} = 0$, $\Delta\Phi_t = 0$, $\text{noise}_{\Phi} = 0$, and $\text{noise}(t)$ is white noise with a maximal amplitude of 0.02 sec.

The upper panel of Fig. 1 shows the power spectrum of the URRI series estimated by the CWT method. The ridge in the power spectrum at the respiratory frequency can be easily distinguished from the LF component (at 0.1 Hz) at all time steps. The lower panels show the

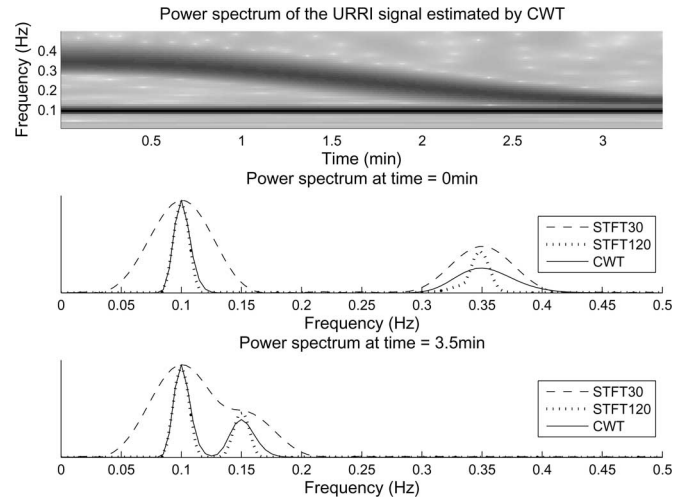


Fig. 1. Synthetic data with a respiratory frequency varying from 0.35 to 0.15 Hz: the first panel shows the power spectrum of the URRI signal estimated by CWT. The ridge at the respiratory frequency can be distinguished from the LF component at 0.1 Hz for all time steps. The second and third panels show the normalized power spectra of the synthetic HRV signal, estimated by STFT30 (dashed line), STFT120 (dotted line), and CWT (plain line), at time 0 min (second panel) and 3.5 min (third panel). In the second panel, for time 0 min, all algorithms are able to distinguish between the two peaks. In the third panel, for time 3.5 min, only STFT120 and CWT give acceptable results.

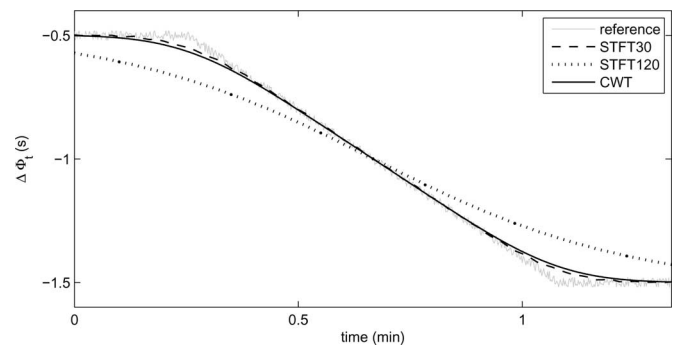


Fig. 2. Synthetic data with a phase delay varying from -0.5 to -1.5 sec, with white noise of maximal amplitude 0.02 sec added to the phase: phase delay $\Delta\Phi_t$ estimated by STFT30 (dashed line), STFT120 (dotted line) and CWT (plain line). STFT30 and CWT are able to track similarly the $\Delta\Phi_t$ variations, while STFT120 performs less accurately.

power spectra obtained by the STFT30, STFT120, and CWT methods, at the beginning and end of the signal. When the frequencies of the two peaks are far from each other, the peaks can be separated by all methods. However, when the respiratory frequency gets closer to the LF – HF frontier, STFT30 fails because the frequency resolution cannot separate the HF peak from the neighboring LF peak.

2) *Time-varying phase delay*: The ability to track phase delays is evaluated on synthetic data with a constant respiratory frequency $f_{\text{resp}} = 0.3$ Hz and a time-varying phase delay. The phase delay expressed in seconds $\Delta\Phi_t(t)$ varies linearly from -0.500 sec to -1.500 sec in 50 sec, between two constant plateaus. noise_{Φ} is white noise with a maximal amplitude of 0.02 sec. The remaining parameters of (2) and (3) are $a_1 = 0.2$, $\Phi_{t0} = 0$, $b_0 = 1$ sec, $b_{\text{VLF}} = 0.07$ sec, $f_{\text{VLF}} = 0.04$ Hz, $b_{\text{LF}} = 0.06$ sec, $f_{\text{LF}} = 0.1$ Hz, $b_{\text{HF}} = 0.06$ sec, and $\text{noise}(t) = 0$.

Fig. 2 shows the phase delay $\Delta\Phi_t(t)$ estimated by STFT30, STFT120, and CWT, together with the reference. STFT30 and CWT

are able to track similarly the $\Delta\Phi_t$ variations, while STFT120 performs less accurately. Indeed, the maximal estimation errors are 0.059, 0.064, and 0.186 sec for STFT30, CWT, and STFT120, respectively. The poor results of STFT120 are due to its low time resolution: results are averaged over the window length.

The algorithm's ability to track fast changes depends on its time resolution. It can be quantified via the rise time of the obtained phase response to an imposed step in the phase delay. For STFT30 and STFT120, the rise time from 10% to 90% of the final value is independent of the respiratory frequency, and equal to 15 and 55 sec, respectively. For CWT, it is equal to 15 sec at $f_{\text{resp}} = 0.35$ Hz, and 34 sec at $f_{\text{resp}} = 0.15$ Hz. These data confirm that CWT and STFT30 perform similarly at high respiratory frequencies, while STFT120 performs worse. Although CWT does not perform as well for low as for high respiratory frequencies, it still outperforms STFT120. For low respiratory frequencies, STFT30 theoretically performs best in tracking changes. However, it is unable to isolate the HF peak.

IV. DISCUSSION AND CONCLUSION

A CWT-based algorithm is presented for the analysis of RSA. The proposed method is compared on synthetic data to STFT-based analyzes using short or long time-windows (30 and 120 sec). These window lengths have been chosen because the first gives the desired time resolution in the HF band, while the second is a standard compromise for studying HRV.

Results on synthetic data show that neither STFT30 nor STFT120 is able to simultaneously and accurately identify low respiratory frequencies and transients. On the one hand, Fourier-based analysis with a short window cannot distinguish between LF and HF peaks in the URRI signal, when the respiratory frequency drops below 0.2 Hz. On the other hand, Fourier-based analysis with a long window is not able to track fast phase delay variations.

Results obtained with the CWT-based method on synthetic data show that the method is able to handle both limitations of the STFT-based algorithms. This is explained by the intrinsic variation of the trade-off between time- and frequency resolutions in CWTs: a low time- and high frequency resolution are used to analyze low frequencies, which allows the detection of the HF component of HRV even for low respiratory frequencies, and a high time- and low frequency resolution to analyze high frequencies, which allows the tracking of fast variations. The proposed method is, therefore, better suited than Fourier-based analyzes for the study of cardiorespiratory interaction dynamics, when low breathing frequencies are present.

REFERENCES

- [1] M. Malik, J. T. Bigger, A. J. Camm, R. E. Kleiger, A. Malliani, A. J. Moss, and P. J. Schwartz, "Heart rate variability: Standards of measurement, physiological interpretation, and clinical use," *Eur. Heart J.*, vol. 17, no. 3, pp. 354–381, 1996.
- [2] S. Akselrod, D. Gordon, F. A. Ubel, D. C. Shannon, A. C. Berger, and R. J. Cohen, "Power spectrum analysis of heart rate fluctuation: A quantitative probe of beat-to-beat cardiovascular control," *Science*, vol. 213, no. 4504, pp. 220–222, 1981.
- [3] M. Piepoli, P. Sleight, S. Leuzzi, F. Valle, G. Spadacini, C. Passino, J. Johnston, and L. Bernardi, "Origin of respiratory sinus arrhythmia in conscious humans: An important role for arterial carotid baroreceptors," *Circulation*, vol. 95, no. 7, pp. 1813–1821, 1997.
- [4] E. Pyetan and S. Akselrod, "Do the high-frequency indexes of HRV provide a faithful assessment of cardiac vagal tone? A critical theoretical evaluation," *IEEE Trans. Biomed. Eng.*, vol. 50, no. 6, pp. 777–783, Jun. 2003.
- [5] J. P. Saul, R. D. Berger, P. Albrecht, S. P. Stein, M. H. Chen, and R. J. Cohen, "Transfer function analysis of the circulation: unique insights into cardiovascular regulation," *AJP: Heart Circ. Physiol.*, vol. 261, no. 4, pp. H1231–1245, 1991.
- [6] W. H. Cooke, J. B. Hoag, A. A. Crossman, T. A. Kuusela, K. U. O. Tahvanainen, and D. L. Eckberg, "Human responses to upright tilt: A window on central autonomic integration," *J. Physiol.*, vol. 517, no. 2, pp. 617–628, 1999.
- [7] P. Migeotte and Y. Verbandt, "A novel algorithm for the heart rate variability analysis of short-term recordings: Polar representation of respiratory sinus arrhythmia," *Comput. Biomed. Res.*, vol. 32, pp. 55–66, 1999.
- [8] S. Cerutti, A. M. Bianchi, and L. T. Mainardi, "Advanced spectral methods for detecting dynamic behaviour," *Auton. Neurosci.*, vol. 90, pp. 3–12, 2001.
- [9] H. Chan, H. Huang, and J. Lin, "Time-frequency analysis of heart rate variability during transient segments," *Annals Biomed. Eng.*, vol. 29, no. 11, pp. 983–996, 2001.
- [10] L. Keselbrener and S. Akselrod, "Selective discrete fourier transform algorithm for time-frequency analysis: Method and application on simulated and cardiovascular signals," *IEEE Trans. Biomed. Eng.*, vol. 43, no. 8, pp. 789–802, Aug. 1996.
- [11] V. Pichot, J. M. Gaspoz, S. Molliex, A. Antoniadis, T. Busso, F. Roche, F. Costes, L. Quintin, J. R. Lacour, and J. C. Barthelemy, "Wavelet transform to quantify heart rate variability and to assess its instantaneous changes," *J. Appl. Physiol.*, vol. 86, pp. 1081–1091, 1999.
- [12] R. Bates, M. Hilton, K. Godfrey, and M. Chappell, "Comparison of methods for harmonic wavelet analysis of heart rate variability," *IEE Proc. Sci. Meas. Tech.*, vol. 145, no. 6, pp. 291–300, 1998.
- [13] A. R. Elliott, S. A. Shea, D. J. Dijk, J. K. Wyatt, E. Riel, D. F. Neri, C. A. Czeisler, J. B. West, and G. K. Prisk, "Microgravity reduces sleep-disordered breathing in humans," *Amer. J. Response Crit. Care Med.*, vol. 164, no. 3, pp. 478–485, 2001.
- [14] A. U. Viola, C. Simon, J. Ehrhart, F. Piquard, A. Muzer, and G. Brandenberger, "Sleep processes exert a predominant influence on the 24-h profile of heart rate variability," *J. Biol. Rhythms*, vol. 17, no. 6, pp. 539–47, Dec. 2002.
- [15] P. S. Addison, *The Illustrated Wavelet Transform Handbook: Introductory Theory and Applications in Science, Engineering, Medicine and Finance*. London, U.K.: Institute of Physics Publishing, 2002.